

L'ANALYSE NUMÉRIQUE ET LA THÉORIE DE L'APPROXIMATION

Tome 7, N° 2, 1978, pp. 193—209

NUMERICAL EVALUATIONS OF COMPRESSIBILITY
CORRECTIONS IN WAKE FLOWS

by

SIMONA POPP

(Bucureşti)

Introduction

The study of compressible fluid flow has been substantiated at the beginning of this century by S. A. CHAPLYGHIN [1] in his well-known doctoral thesis, in which he gives two research methods, an exact one and an approximate one. Both methods are hodograph methods. This means that one should use the independent variables V and θ (V is the magnitude of the velocity vector and θ the angle made by this vector with a certain direction).

Chaplygin's methods led subsequently to numerous and important investigations in the field [2], [3]. However, his exact method and its extension due to S. V. FALKOVICH [4] can be applied only to some classes of motion and imply laborious calculations.

In addition, to the advantage of linearizing the system of motion equations, the hodograph method has some disadvantages related to the passing from the hodograph plane to the physical plane.

Therefore, it was necessary to use approximate methods which operate in the physical plane, that is the so-called direct methods.

One of the most interesting methods of this kind, which can be applied to various classes of motion is that given by I. IMAI [5], E. LAMBA [6] and C. JACOB [7].

With this method and with other numerous remarkable investigations, C. JACOB inscribed Romania among the first countries which contributed substantially to the study of compressible flows even since 1933—1934, [8], [9], [10], [11], [12].

The Imai-Lamba-Jacob method has been adapted to the examination of configurations which imply wakes [2], [3].

In the following, we shall briefly present the Imai-Lamba-Jacob method and emphasize particularly the formulas we have obtained in a previous work by using this method [2].

Particular stress will be laid on the expressions of the drag and lift coefficients in wake problems in an unbounded fluid in which a wedge-shaped body or a flat plate inclined with respect to the stream velocity at infinity upstream, is placed.

The numerical values of the above coefficients are listed in tables and diagrams and compared to similar values corresponding to the incompressible fluid.

The purpose of this paper is to estimate, numerically, the compressibility effects on various motion elements.

1. The Imai-Lamba-Jacob method

We consider the bidimensional, subsonic, steady, irrotational motion of a compressible fluid subjected to the isentropic law,

$$(1.1) \quad \frac{p}{p_0} = \left(\frac{\rho}{\rho_0} \right)^\gamma$$

p and ρ being the fluid pressure and specific mass, respectively, p_0 and ρ_0 the same quantities for zero velocity and $\gamma = c_p/c_v$ (c_p is the specific heat under constant pressure and c_v the specific heat at constant volume). Let $\varphi(x, y)$ be the velocity potential, $\psi(x, y)$ the stream function, $u(x, y)$ and $v(x, y)$ the projections of the velocity \vec{V} on the orthogonal coordinate axes Ox and Oy in the motion plane (Ox has the same direction as that of the velocity vector at infinity upstream).

By virtue of the fundamental system

$$(1.2) \quad \frac{\partial \varphi}{\partial x} = \frac{\rho_0}{\rho} \frac{\partial \psi}{\partial y}, \quad \frac{\partial \varphi}{\partial y} = - \frac{\rho_0}{\rho} \frac{\partial \psi}{\partial x}$$

we obtain the relation,

$$(1.3) \quad \frac{\partial f}{\partial \bar{z}} = \frac{1 - \frac{\rho}{\rho_0} \frac{\partial \bar{f}}{\partial \bar{z}}}{1 + \frac{\rho}{\rho_0} \frac{\partial \bar{f}}{\partial \bar{z}}}$$

by introducing the functions $f(z, \bar{z}) = \varphi + i\psi$, $\bar{f}(z, \bar{z}) = \varphi - i\psi$ with $z = x + iy$ and $\bar{z} = x - iy$.

The function f and \bar{f} can be expanded in the following power series,

$$(1.4) \quad f(z, \bar{z}) = f_0 + M_\infty^2 f_1 + M_\infty^4 f_2 + \dots$$

$$\bar{f}(z, \bar{z}) = \bar{f}_0 + M_\infty^2 \bar{f}_1 + M_\infty^4 \bar{f}_2 + \dots$$

where $M_\infty = \frac{V_\infty}{c_\infty}$ is the Mach number.

By replacing (1.4) into (1.3) and equalizing the coefficients of the same powers of M_∞ we deduce the relations,

$$f_0 = f_0(z) = \varphi_0(x, y) + i\psi_0(x, y),$$

$$f_1(z, \bar{z}) = \varphi_1(x, y) + i\psi_1(x, y) =$$

$$= \frac{1}{4v_\infty^2} \frac{df_0}{dz} \int_{z_0}^z \left(\frac{df_0}{dz} \right)^2 dz + \frac{1}{4} g(z)$$

$$f_2(z, \bar{z}) = \varphi_2(x, y) + i\psi_2(x, y) = \dots$$

where the functions $f_0(z)$ and $g(z)$ are analytical functions of z which can be determined by using the boundary conditions specific to problems under examination. In the problems of Helmholtz type we shall be concerned with, the function $f_0(z)$ will be chosen as complex potential of the incompressible motion corresponding to the same walls and the same velocity at infinity upstream as in the compressible motion.

The function $g(z)$ will be determined through the intermedium of another function $g_1(z) = g(z) + f_0(z)$, that is the determination reduces finally to the solution of a boundary problem of mixed type.

Once the function $f_0(z)$ and $g(z)$ are obtained, various motion elements can be calculated.

Detailed researches in this respect have been carried out in my papers [2], [3].

2. Expression of the drag coefficient for the wedgeshaped body

We consider the wedge P_1OP_2 ($OP_1 = OP_2 = l$) with an included angle of 2μ , situated in a subsonic, unbounded flow with the velocity \vec{V}_∞ at infinity upstream. From the ends P_1 and P_2 the free lines λ_1 and λ_2 separate (Fig. 1).

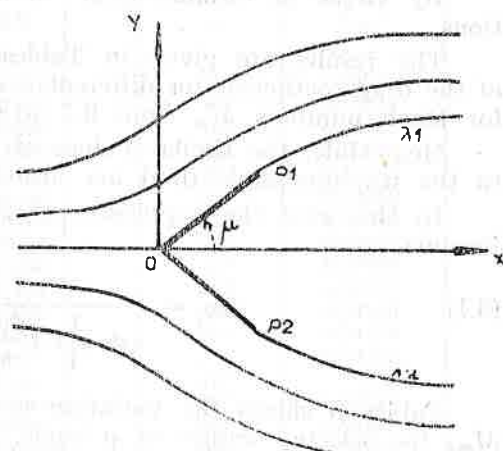


Fig. 1

The drag coefficient C_D is defined by the relation,

$$C_D = \frac{R_x}{\rho_\infty V_\infty^2 l \sin \mu} \quad (2.1)$$

where R_x represents the resultant of the aerodynamic forces acting on the body in the Ox direction, R_y being equal to zero due to the configuration symmetry.

Using the Imai-Lamba-Jacob method and taking account of relation (2.1), in paper [2] we have obtained the expression of C_D under the form,

$$(2.2) \quad C_D = \frac{4\mu^2}{\pi \sin \mu \left[1 + \frac{2\mu}{\pi} + \frac{4\mu^2}{\pi^2} \beta \left(1 - \frac{\mu}{\pi} \right) \right]} \times \\ \times \left\{ 1 + M_\infty^2 \frac{\pi \sin \mu \left[1 + \frac{2\mu}{\pi} + \frac{4\mu^2}{\pi^2} \beta \left(1 - \frac{\mu}{\pi} \right) \right] - 2\mu^2}{2\pi \sin \mu \left[1 + \frac{2\mu}{\pi} + \frac{4\mu^2}{\pi^2} \beta \left(1 - \frac{\mu}{\pi} \right) \right]} \right\}$$

where $\beta(x)$ is the Stirling function,

$$(2.3) \quad \beta(x) = \sum_{n=0}^{\infty} (-1)^n \frac{1}{n+x}$$

3. Numerical results

By virtue of formula (2.2) we have carried out numerical calculations.

The results are given in Tables 1, 2 and 3, which include values of the drag coefficient for different μ angles varying from 5° to 90° and for Mach numbers M_∞ from 0.1 to 0.9.

Meanwhile, the similar values of the drag coefficients corresponding to the incompressible fluid are also listed in the table 4.

In this case the expression of the drag coefficient is given by the formula,

$$(3.1) \quad C_{D_i} = \frac{4\mu^2}{\pi \sin \mu \left[1 + \frac{2\mu}{\pi} + \frac{4\mu^2}{\pi^2} \beta \left(1 - \frac{\mu}{\pi} \right) \right]}$$

Tables 5 shows the variation of the coefficient C_D with respect to M_∞ , for selected values of μ angle.

These tables are accompanied by the diagrams given in figures 2 and 3.

These tables are accompanied by the diagrams given in figures 2 and 3.

TABLE 1
 C_D

$\mu \backslash M_\infty$	0.1	0.2	0.3
5°	0.10568	0.10716	0.10966
10°	0.20028	0.20296	0.20746
15°	0.28504	0.28870	0.29480
20°	0.36102	0.36548	0.37290
25°	0.42922	0.23432	0.44284
30°	0.49044	0.49610	0.50554
35°	0.54542	0.55156	0.56180
40°	0.59484	0.60140	0.61234
45°	0.63924	0.64620	0.65778
50°	0.67908	0.68650	0.69870
55°	0.71508	0.72278	0.73558
60°	0.74738	0.75544	0.76884
65°	0.77642	0.78496	0.79890
70°	0.80256	0.81138	0.82610
75°	0.82604	0.83530	0.85074
80°	0.84716	0.85690	0.87314
85°	0.86616	0.87742	0.89354
90°	0.88324	0.89410	0.91220

TABLE 2
 C_D

$\mu \backslash M_\infty$	0.4	0.5	0.6
5°	0.11314	0.11762	0.12314
10°	0.21374	0.22184	0.23172
15°	0.30336	0.31434	0.32798
20°	0.38330	0.39668	0.41302
25°	0.45476	0.47010	0.48884
30°	0.51874	0.53574	0.55650
35°	0.57612	0.59454	0.61706
40°	0.62766	0.64734	0.67142
45°	0.67402	0.69488	0.72036
50°	0.71570	0.73776	0.76460
55°	0.75350	0.77656	0.80472
60°	0.78762	0.81178	0.84128
65°	0.81856	0.84384	0.87476
70°	0.84670	0.87318	0.90556
75°	0.87236	0.90016	0.93412
80°	0.89588	0.92510	0.96082
85°	0.90752	0.94832	0.98598
90°	0.93756	0.97016	1.01000

TABLE 3
 C_D

$\mu \backslash M_\infty$	0.7	0.8	0.9
5°	0.12592	0.13706	0.14552
10°	0.24340	0.25688	0.27214
15°	0.34366	0.36200	0.38276
20°	0.43232	0.45460	0.47986
25°	0.51098	0.53654	0.56550
30°	0.58104	0.60936	0.64024
35°	0.64366	0.67436	0.70916
40°	0.69986	0.73268	0.76988
45°	0.75050	0.78526	0.82466
50°	0.79634	0.83294	0.87444
55°	0.83802	0.87644	0.91998
60°	0.87616	0.91640	0.96202
65°	0.91126	0.95340	1.00116
70°	0.94382	0.98798	1.03800
75°	0.97426	1.02058	1.07308
80°	1.00302	1.05172	1.10692
85°	1.03050	1.08184	1.14006
90°	1.05710	1.11142	1.17300

TABLE 4

μ	C_{D_i}
5°	0.10518
10°	0.19938
15°	0.28382
20°	0.35954
25°	0.42752
30°	0.48856
35°	0.54340
40°	0.59268
45°	0.63698
50°	0.67680
55°	0.71260
60°	0.74478
65°	0.77372
70°	0.79972
75°	0.82310
80°	0.84408
85°	0.86290
90°	0.87980

TABLE 5
 C_D

$M_\infty \backslash \mu$	15°	30°	45°	60°	75°	90°
0.10	0.28504	0.49044	0.63924	0.74738	0.82604	0.88324
0.15	0.28656	0.49280	0.64214	0.75074	0.82890	0.88776
0.20	0.28870	0.49610	0.64620	0.75544	0.83530	0.89410
0.25	0.29144	0.50034	0.65142	0.76146	0.84226	0.90224
0.30	0.29480	0.50554	0.65778	0.76884	0.85274	0.91220
0.35	0.29878	0.51166	0.66532	0.77756	0.86078	0.92398
0.40	0.30336	0.51874	0.67402	0.78762	0.87236	0.93756
0.45	0.30854	0.52678	0.68386	0.79902	0.88428	0.95296
0.50	0.31434	0.53574	0.69488	0.81178	0.90016	0.97016
0.55	0.32076	0.54564	0.70704	0.82586	0.91636	0.98918
0.60	0.32778	0.55650	0.72036	0.84128	0.93412	1.01000
0.65	0.33542	0.56830	0.73486	0.85806	0.95342	1.03264
0.70	0.34366	0.58104	0.75050	0.87616	0.97426	1.05708
0.75	0.35252	0.59472	0.76730	0.89562	0.99666	1.08334
0.80	0.36200	0.60936	0.78526	0.91640	1.02058	1.11142
0.85	0.37208	0.62492	0.80438	0.93854	1.04606	1.14130
0.90	0.38276	0.64144	0.82466	0.96202	1.07208	1.17300

From all tables and diagrams the following conclusions can be drawn:

1. The drag coefficient increases with the increase of the μ angle reaching a maximum value for $\mu = 90^\circ$.
2. For any angle μ the drag coefficient C_D increases with the increase of the Mach number M_∞ .
3. The drag coefficient for a body placed in a compressible fluid is always higher than that corresponding to the incompressible fluid and the difference between the respective coefficients increases with the increase of the angle μ and M_∞ . (Fig. 3)

4. Inclined Flat Plate

We consider a flat plate $P_1 P_2 = l$ placed in an unbounded compressible fluid (fig. 4).

The plate is inclined by an angle α with respect to the direction of the fluid velocity V_∞ .

In the physical plane we consider a reference system Oxy with the origin at the stagnation point O on the plate.

The Ox -axis has the direction of V_∞ and the Oy -axis is perpendicular to it.

From the edges P_1 and P_2 of the plate two free streamlines λ_1 and λ_2 separate.

The normal to the plate forms with Ox -axis the angle δ .

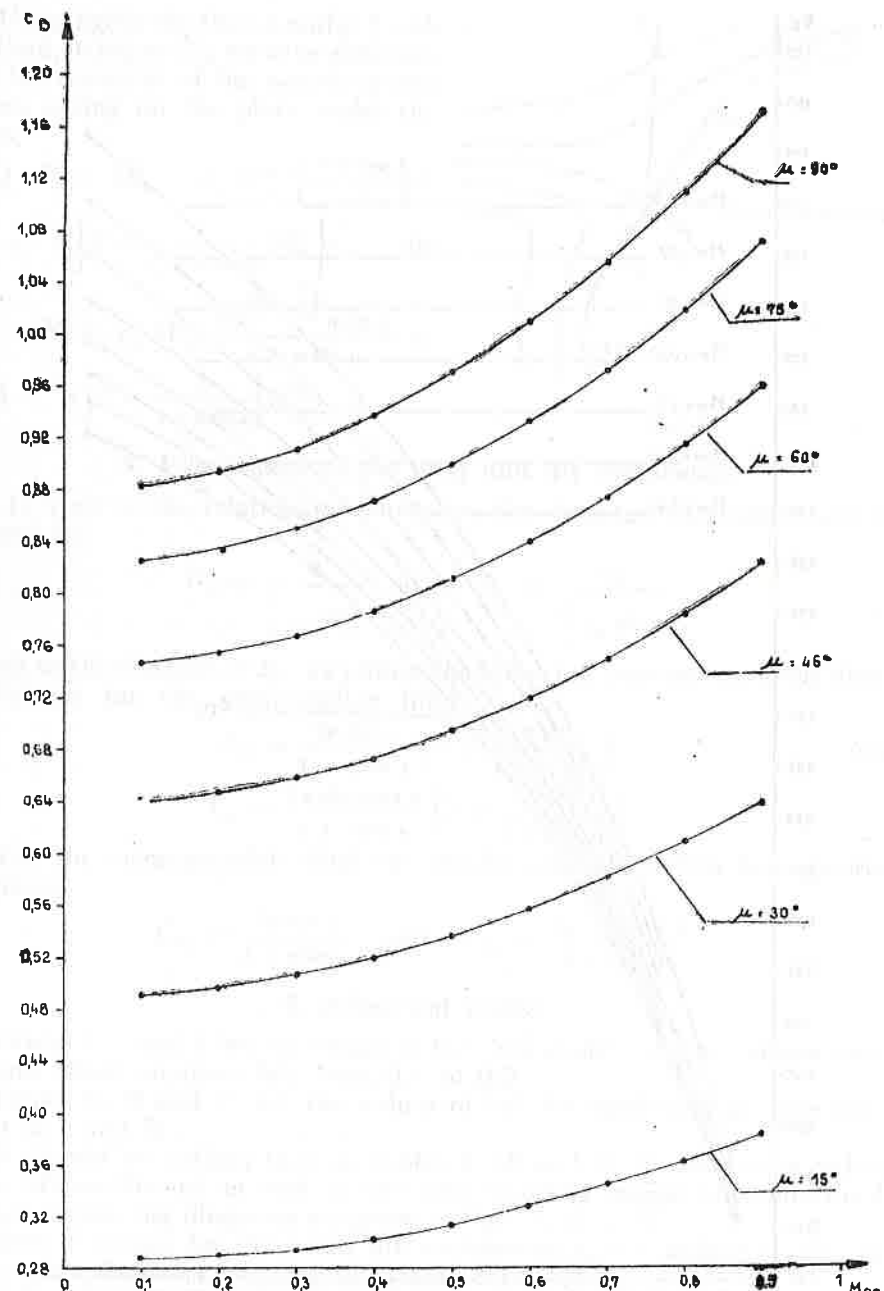


Fig. 2.

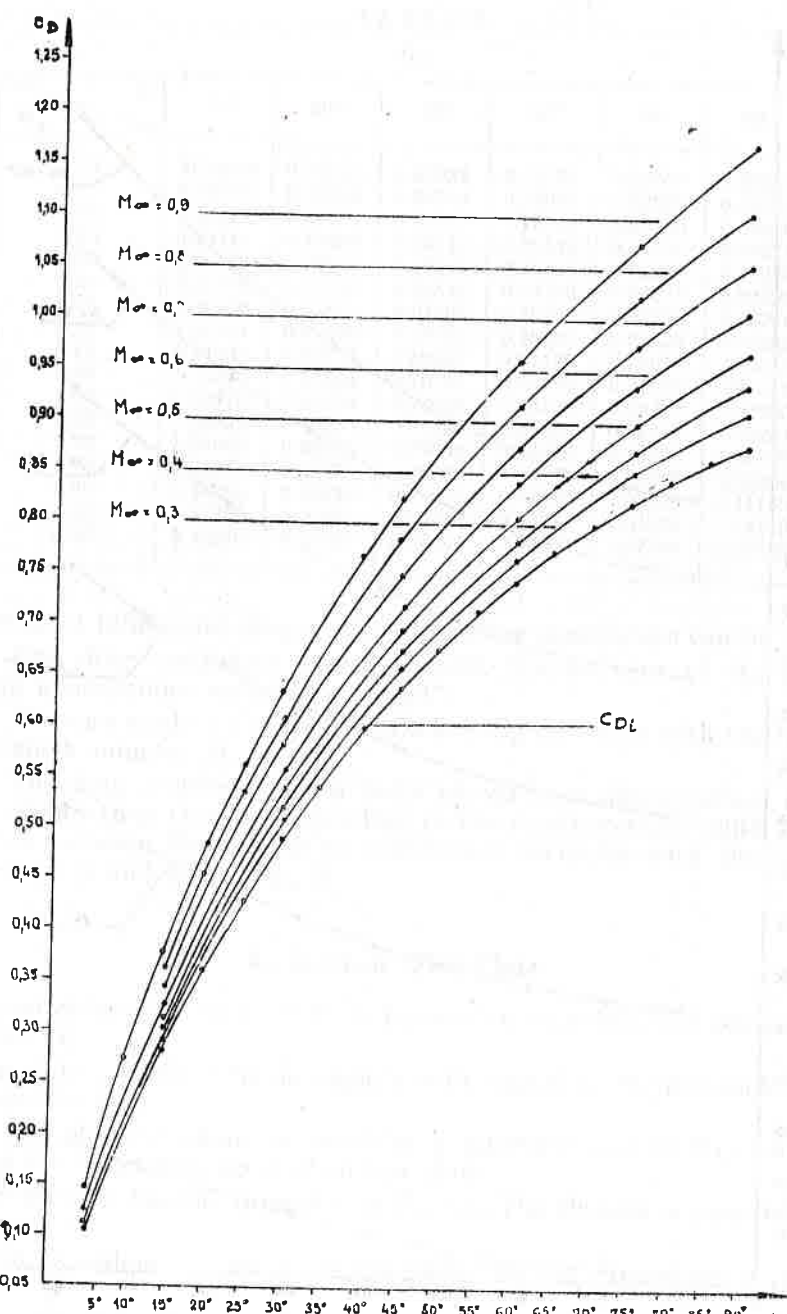


Fig. 3.

Using again the Imai-Lamba-Jacob method, in paper [2], we have determined the resultant of the aerodynamics forces acting on the plate under the form,

$$(4.1) \quad R_x - iR_y = \rho_\infty l V_\infty^2 \frac{e^{-i\delta} \pi \cos \delta}{4 + \pi \cos \delta} \times \\ \times \left[1 + \frac{2}{4 + \pi \cos \delta} M_\infty^2 \right], \quad \text{or}$$

$$R_x - iR_y = \rho_\infty l V_\infty^2 \frac{e^{-i(\alpha - \frac{\pi}{2})} \pi \sin \alpha}{4 + \pi \sin \alpha} \times \\ \times \left[1 + \frac{2}{4 + \pi \sin \alpha} \right] M_\infty^2.$$

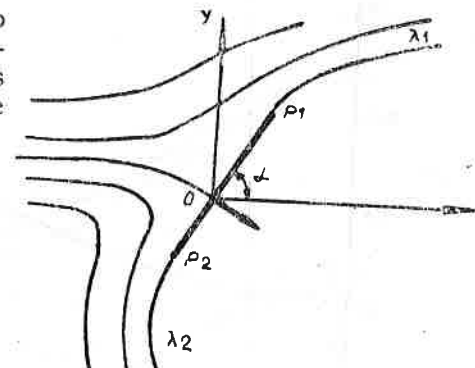


Fig. 4

5. Expressions of the drag and lift coefficients

In view of the relations which define the drag and lift coefficients expressed by,

$$(5.1) \quad C_D = \frac{R_x}{\frac{1}{2} \rho_\infty V_\infty^2 l} \quad \text{and} \quad C_L = \frac{R_y}{\frac{1}{2} \rho_\infty V_\infty^2 l}$$

as well as the relation (4.2), we obtain the following expressions of the above coefficients for the compressible fluid

$$(5.2) \quad C_D = \frac{2\pi \sin^2 \alpha}{4 + \pi \sin \alpha} \left(1 + \frac{2M_\infty^2}{4 + \pi \sin \alpha} \right) \quad \text{and}$$

$$(5.3) \quad C_L = \frac{2\pi \sin \alpha \cos \alpha}{4 + \pi \sin \alpha} \left(1 + \frac{2M_\infty^2}{4 + \pi \sin \alpha} \right)$$

For the incompressible fluid the similar coefficients can be expressed as follows :

$$(5.4) \quad C_{D_i} = \frac{2\pi \sin^2 \alpha}{4 + \pi \sin \alpha} \quad \text{and} \quad C_{D_i} = \frac{2\pi \sin \alpha \cos \alpha}{4 + \pi \sin \alpha}$$

6. Numerical results

Tables 6, 7 and 8 list the values of the drag coefficient for various α -angles and Mach numbers M_∞ from 0.1 to 0.9.

Tables 9, 10 and 11 list the values of the lift coefficient for the same values of α and M_∞ .

It should be noticed that in Tables 9, 10 and 11 the maximum values of the lift coefficient as well as the corresponding angles are underlined.

Accompanying diagrams are given in figs. 5, 6, 7, 8.

Similar values for drag and lift coefficients corresponding to the incompressible fluid are included in tables 12 and 13.

Tables 14 and 15 list the values of C_D and C_L for selected values of μ angles and M_∞ varying from 0.05 to 0.90.

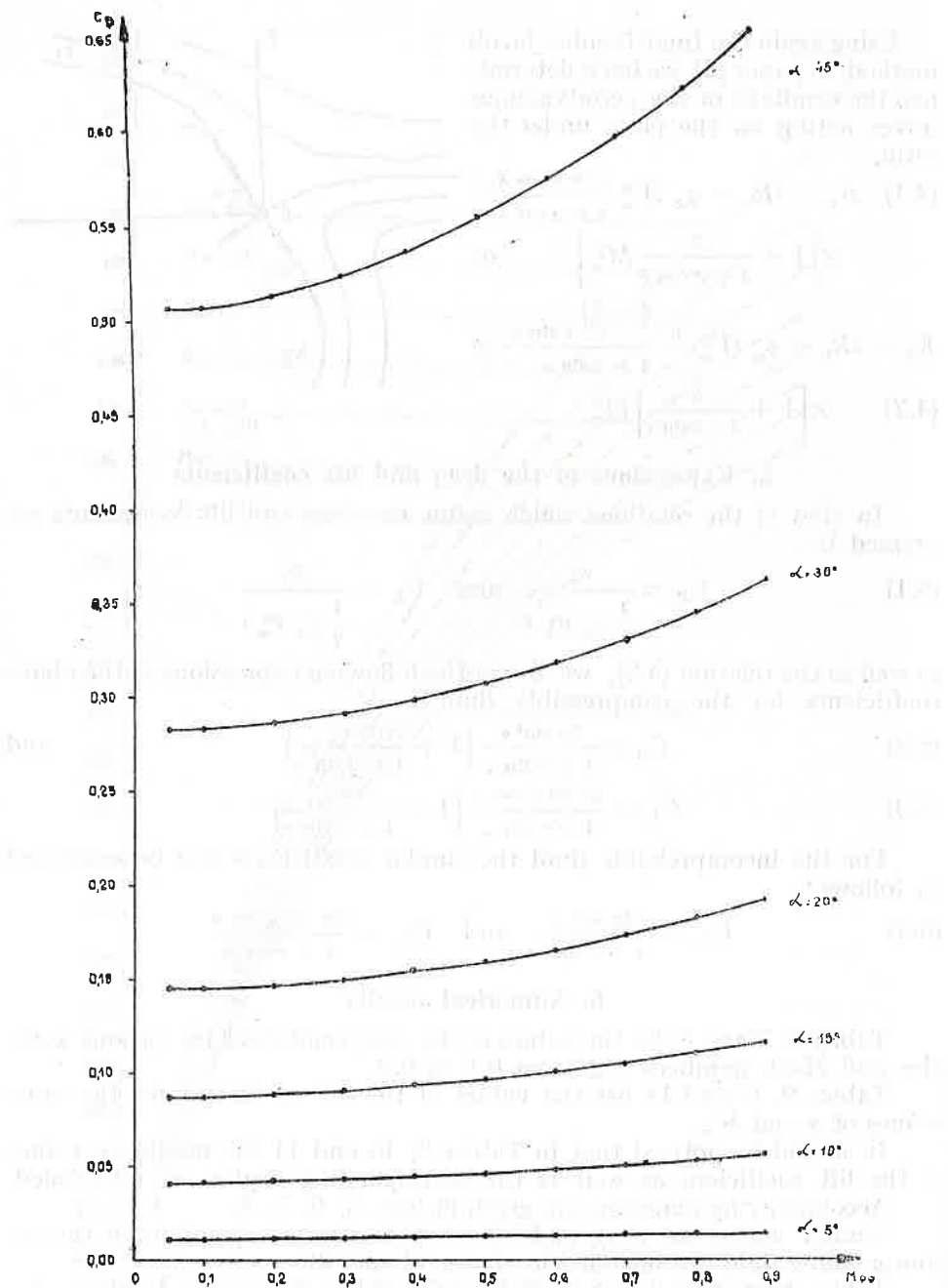


Fig. 5.

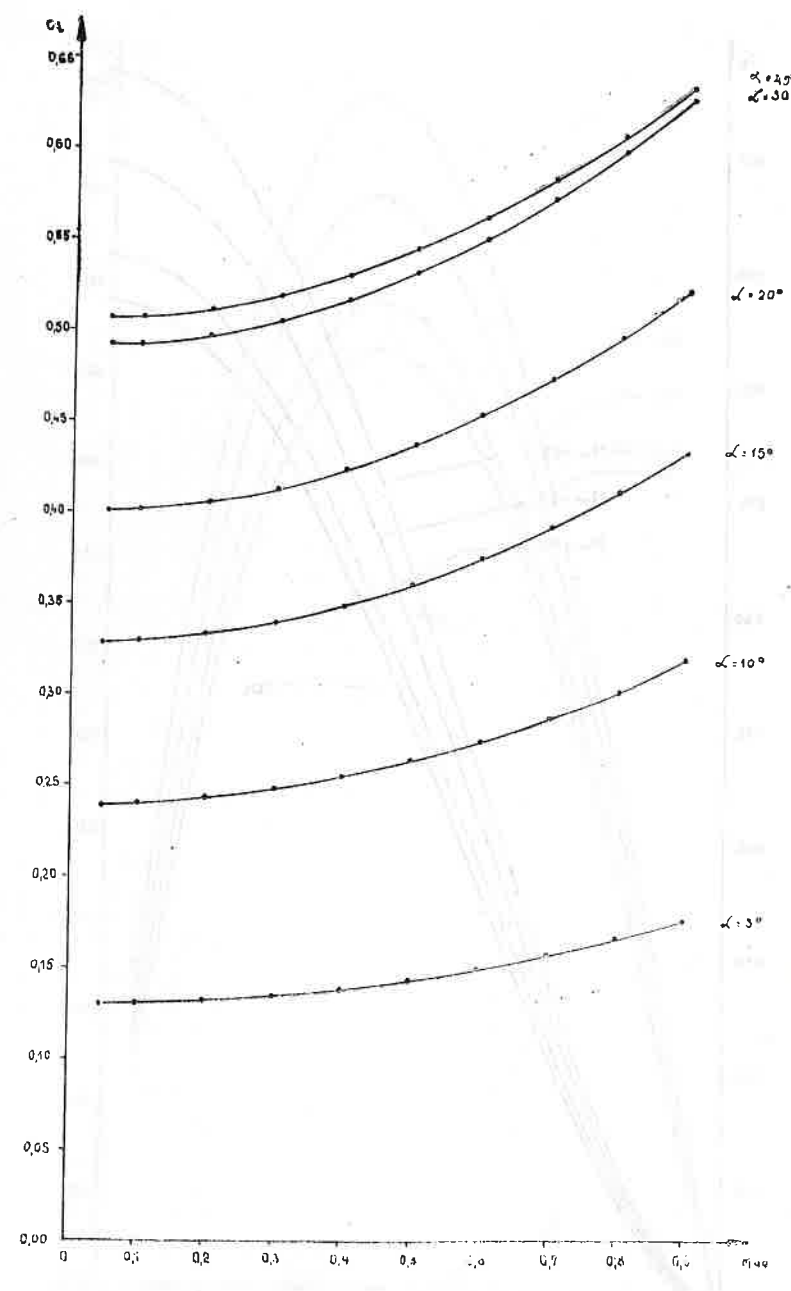


Fig. 6.

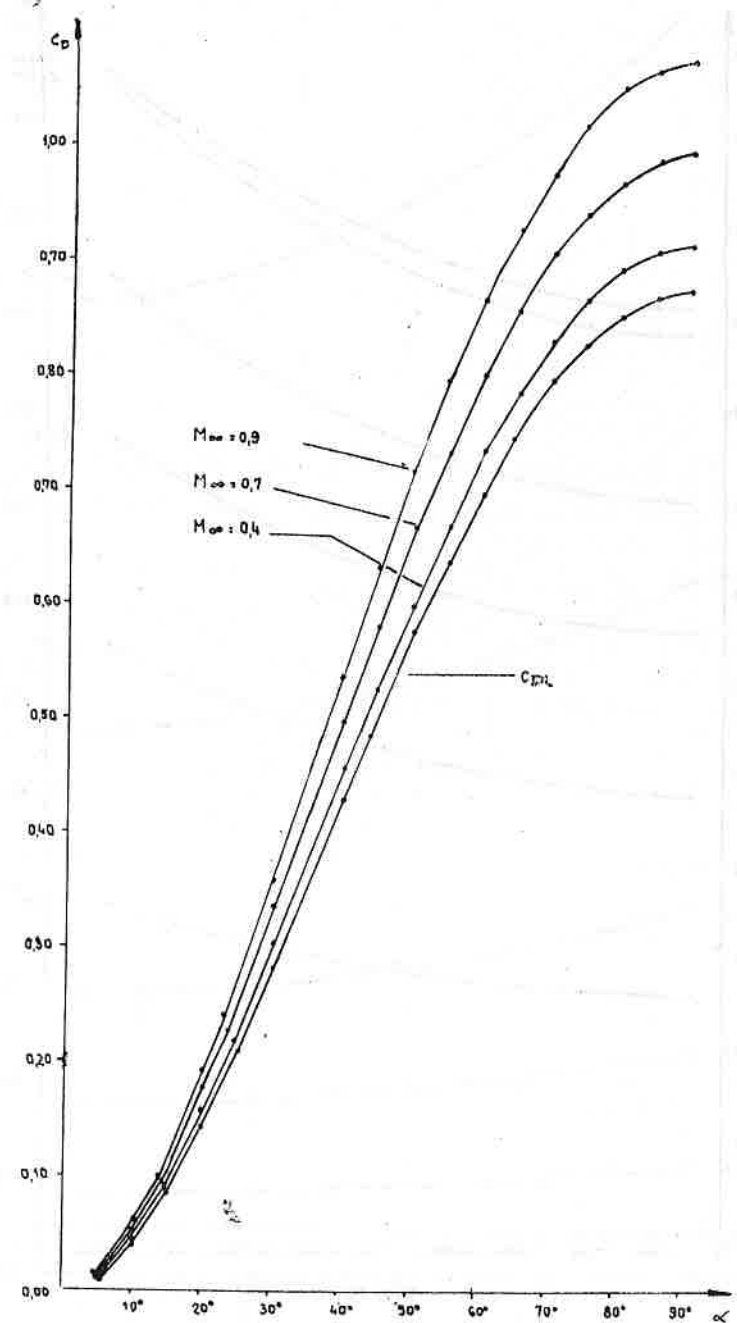


Fig. 7.

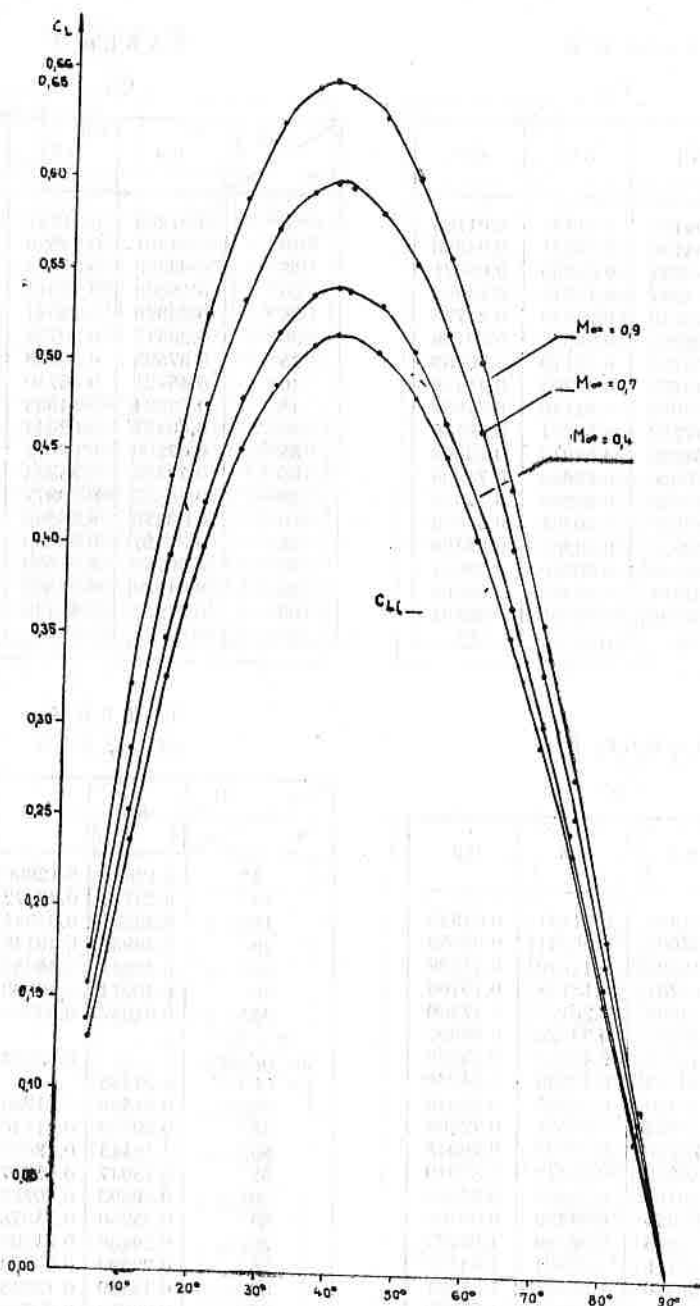


Fig. 8.

TABLE 6

 C_D

$M_\infty \backslash \alpha$	0.1	0.2	0.3
5°	0.01122	0.01137	0.01163
10°	0.04186	0.04241	0.04333
15°	0.08781	0.08890	0.09071
20°	0.14541	0.14712	0.14998
25°	0.21143	0.21380	0.21776
30°	0.28298	0.28602	0.29108
35°	0.35751	0.36119	0.36733
40°	0.43272	0.43702	0.44418
45°	0.50659	0.51146	0.51957
50°	0.57732	0.58271	0.59169
55°	0.64333	0.64919	0.65894
60°	0.70326	0.70952	0.71995
65°	0.75593	0.76254	0.77354
70°	0.80035	0.80724	0.81872
75°	0.83573	0.84284	0.85468
80°	0.86144	0.86870	0.88081
85°	0.87704	0.88440	0.89666
90°	0.88226	0.88966	0.90197

TABLE 7

 C_D

$M_\infty \backslash \alpha$	0.4	0.5	0.6
5°	0.01200	0.01247	0.01305
10°	0.04461	0.04626	0.04828
15°	0.09326	0.09653	0.10053
20°	0.15398	0.15911	0.16540
25°	0.22329	0.23041	0.23910
30°	0.29817	0.30728	0.31841
35°	0.37593	0.38698	0.40050
40°	0.45421	0.46710	0.48287
45°	0.53094	0.54555	0.56340
50°	0.60427	0.62044	0.64020
55°	0.67260	0.69017	0.71163
60°	0.73456	0.75334	0.77629
65°	0.78895	0.80877	0.83298
70°	0.83479	0.85545	0.88070
75°	0.87127	0.89259	0.91865
80°	0.89776	0.91956	0.9420
85°	0.91384	0.93592	0.96290
90°	0.91922	0.94140	0.96850

TABLE 10

 C_L

$M_\infty \backslash \alpha$	0.4	0.5	0.6
5°	0.13720	0.14258	0.14915
10°	0.25302	0.26239	0.27383
15°	0.34806	0.36026	0.37518
20°	0.42304	0.43716	0.45441
25°	0.47885	0.49411	0.51276
30°	0.51644	0.53222	0.55151
35°	0.53688	0.55267	0.57196
38°34' 8"	—	—	0.57611
38°45' 56"	—	0.55715	—
38°56' 7"	0.54165	—	—
40°	0.54131	0.55668	0.57546
45°	0.53094	0.54555	0.56340
50°	0.50704	0.52061	0.53719
55°	0.47096	0.48326	0.49829
60°	0.42410	0.43494	0.44819
65°	0.36790	0.37713	0.38843
70°	0.30384	0.31136	0.32055
75°	0.23346	0.23917	0.24615
80°	0.15830	0.16214	0.16684
85°	0.07995	0.08188	0.08424

TABLE 11

 C_L

$M_\infty \backslash \alpha$	0.7	0.8	0.9
5°	0.15691	0.16588	0.17603
10°	0.28735	0.30295	0.32063
15°	0.39281	0.41315	0.43620
20°	0.47480	0.49833	0.52499
25°	0.53481	0.56024	0.58907
30°	0.57430	0.60060	0.63041
35°	0.59476	0.62107	0.65089
37°52' 24"	—	—	0.65392
38°7' 3"	—	0.62449	—
38°21' 4"	0.59856	—	—
40°	0.59766	0.62328	0.65231
45°	0.58450	0.60885	0.63645
50°	0.55679	0.57940	0.60503
55°	0.51605	0.53655	0.55978
60°	0.46385	0.48193	0.50241
65°	0.40177	0.41717	0.43462
70°	0.33141	0.34395	0.35815
75°	0.25441	0.26393	0.27472
80°	0.17239	0.17880	0.18606
85°	0.08703	0.09025	0.09390

TABLE 8

 C_D

$M_\infty \backslash \alpha$	0.7	0.8	0.9
5°	0.01373	0.01451	0.01540
10°	0.05067	0.05341	0.05653
15°	0.10525	0.11070	0.11688
20°	0.17281	0.18138	0.19108
25°	0.24938	0.26125	0.27469
30°	0.33157	0.34676	0.36397
35°	0.41646	0.43488	0.45576
40°	0.50150	0.52299	0.54736
45°	0.58450	0.60885	0.63645
50°	0.66355	0.69051	0.72105
55°	0.73700	0.76627	0.79945
60°	0.80342	0.83472	0.87019
65°	0.86160	0.89463	0.93205
70°	0.91055	0.94499	0.98402
75°	0.94945	0.98499	1.02527
80°	0.97768	1.01401	1.05518
85°	0.99480	1.03160	1.07331
90°	1.0005	1.03749	1.07938

 C_L

$M_\infty \backslash \alpha$	0.1	0.2	0.3
5°	0.12824	0.12899	0.13302
10°	0.23742	0.23872	0.24574
15°	0.32771	0.32941	0.33856
20°	0.39952	0.40148	0.41206
25°	0.45341	0.45553	0.46698
30°	0.49014	0.49233	0.50417
35°	0.51057	0.51276	0.52460
39°4' 24"	—	—	0.52961
39°10' 32"	—	0.52101	—
39°14' 17"	0.51586	—	—
40°	0.51569	0.51783	0.52935
45°	0.50659	0.51146	0.51957
50°	0.48443	0.48631	0.49649
55°	0.45047	0.45217	0.46140
60°	0.40603	0.40753	0.41567
65°	0.35250	0.35378	0.36071
70°	0.29130	0.29235	0.29799
75°	0.22393	0.22473	0.22901
80°	0.15189	0.15243	0.15531
85°	0.07673	0.07700	0.07845

TABLE 12

 C_{D_i}

α	C_{D_i}	α	C_{D_i}
5°	0.01116	50°	0.57552
10°	0.04168	55°	0.64138
15°	0.08745	60°	0.70117
20°	0.14484	65°	0.75373
25°	0.21064	70°	0.79806
30°	0.28197	75°	0.83335
35°	0.35627	80°	0.85901
40°	0.43128	85°	0.87458
45°	0.50496	90°	0.87980

TABLE 13

 C_{L_i}

α	C_{L_i}	α	C_{L_i}
5°	0.12765	45°	0.50496
10°	0.23638	50°	0.48292
15°	0.32636	55°	0.44910
20°	0.39795	60°	0.40482
25°	0.45172	65°	0.35147
30°	0.48839	70°	0.29047
35°	0.50882	75°	0.22330
39°15' 11"	0.51414	80°	0.15147
40°	0.51398	85°	0.07652

TABLE 14

C_D

M_∞	α	5°	10°	15°	20°	30°
0.05		0.01118	0.04173	0.08754	0.14498	0.28222
0.10		0.01122	0.04186	0.08781	0.14541	0.28298
0.15		0.01128	0.04209	0.08826	0.14612	0.28425
0.20		0.01138	0.04242	0.08890	0.14712	0.28602
0.25		0.01149	0.04283	0.08972	0.14841	0.28826
0.30		0.01164	0.04333	0.09072	0.14998	0.29108
0.35		0.011808	0.04393	0.09190	0.15183	0.29437
0.40		0.01200	0.04462	0.09326	0.15398	0.29817
0.45		0.01223	0.04540	0.09481	0.15640	0.30247
0.50		0.012474	0.04627	0.09653	0.15911	0.30728
0.55		0.01275	0.04723	0.09844	0.16211	0.31259
0.60		0.01305	0.04828	0.10053	0.16539	0.31841
0.65		0.01337	0.04943	0.10280	0.16896	0.32474
0.70		0.013728	0.05066	0.10525	0.17281	0.33157
0.75		0.014107	0.05200	0.10789	0.17695	0.33891
0.80		0.01451	0.05342	0.11070	0.18138	0.34676
0.85		0.01494	0.05493	0.11370	0.18609	0.35511
0.90		0.01540	0.05654	0.11688	0.19108	0.36397

TABLE 15

C_L

M_{∞}	α	5°	10°	15°	20°	30°
0.05		0.12779	0.23664	0.32669	0.39833	0.48882
0.10		0.12824	0.23742	0.32772	0.39952	0.49014
0.15		0.12899	0.23872	0.32941	0.40148	0.49233
0.20		0.13003	0.24054	0.33178	0.40422	0.49540
0.25		0.13138	0.24288	0.33483	0.40775	0.49935
0.30		0.13302	0.24574	0.33856	0.41206	0.50416
0.35		0.13496	0.24912	0.34297	0.41716	0.50987
0.40		0.13720	0.25303	0.34806	0.42304	0.51644
0.45		0.13974	0.25745	0.35382	0.42971	0.52389
0.50		0.14258	0.26238	0.36026	0.43716	0.53222
0.55		0.14572	0.26785	0.36738	0.44539	0.54143
0.60		0.14915	0.27383	0.37518	0.45441	0.55151
0.65		0.15288	0.28033	0.38365	0.46421	0.56247
0.70		0.15692	0.28735	0.39281	0.47480	0.57430
0.75		0.16125	0.29489	0.40264	0.48617	0.58701
0.80		0.16588	0.30295	0.41325	0.49833	0.60060
0.85		0.17080	0.31153	0.42434	0.51127	0.61507
0.90		0.17603	0.32063	0.43621	0.52499	0.63041

REFERENCES

- [1] Chaygin, S. A., *Gas jets*. Collected Works, vol. 2, Moscow, 1948, pp. 19–131.

[2] Pop, S., *Cercetări asupra determinării corecțiilor de compresibilitate la mișcări plane în regim subsonic*. (Researches on the determination of compressibility corrections for subsonic plane flows). Studii și cercetări matematice 1, 1961, pp. 37–90.

[3] Pop, S., *Corrections de compressibilité dans le problème du bilame symétrique*. Comptes rendus Acad. Sci. Paris, t. 249, pp. 619–621 (1959).

[4] Falkovich, S. V., *About Gas jets Theory*, Prikladnaja Matematika i Mekhanika (Translated as: J. Appl. Math. Mech.), vol 21, pp. 459–464 (1957).

[5] Imai, I., Proceedings of the Physico-Math. Soc. of Japan, t. 24, pp. 120–129 (1942).

[6] Lambla, E., *Luftfahrtforschung*, 19, 358–362 (1942).

[7] Jacob, C., *Sur la méthode approchée de M. Lamba en Dynamique des fluides compressibles*. Bull. Sect. Sci. Acad. Roum. Bucureşti, XXVIII pp. 637–641 (1945).

[8] Jacob, C., *Sur quelques problèmes concernant l'écoulement des fluides parfaits compressibles*. Comptes rendus, Acad. Sci. Paris, t. 197, pp. 125–127 (1933).

[9] Jacob, C., *Sur un problème concernant les jets gazeux*. Mathematica, Cluj, vol 8, pp. 205–211 (1934).

[10] Jacob, C., *Introduction mathématique à la Mécanique des fluides*. Ed. Acad. R.P.R. — Gauthier-Villars, Bucarest-Paris, 1959.

[11] Jacob, C., *De l'influence de la compressibilité sur les écoulements fluides*. Disquisitiones Mathematicae et Physicae, t. 6, pp. 193–223 (1947).

[12] Jacob, C., *Actes du IX-e Congrès International de Mécanique appliquée*, t. I. 1957, pp. 464–475 (1957).

[13] Tricomi F. G., *Atti della 2-a Riunione del Groupement de Mathématiciens d'expression latine*. Firenze, 26–30 settembre, 1961, Bologna, 1–3 ottobre 1961. Edizioni Cremonese, Roma (1963), p. 258.

[14] Gurevici, M. I., *Teorija tichenij so sovobodnynei poverlinosteami*. Itogi nauki, Gidromechanika, t. V, p. 63. Moskva. 1971.

Received 7 V 1978

*Institutul Politehnic
Bucuresti*